

Theory of the nonplanar splitting of screw dislocations in Gum Metal

S. V. Bobylev,¹ T. Ishizaki,² S. Kuramoto,² and I. A. Ovid'ko¹

¹*Institute of Problems of Mechanical Engineering, Russian Academy of Sciences, Bolshoj 61, Vasilievskii Ostrov, St. Petersburg 199178, Russia*

²*Toyota Central Research and Development Laboratories Incorporated, Nagakute, Aichi 480-1192, Japan*
(Received 14 August 2007; revised manuscript received 17 December 2007; published 12 March 2008)

A theoretical model is suggested that describes nonplanar splitting of perfect dislocations into partials in a newly discovered group of alloys called Gum Metal. Within the model, the partials have line cores located at a nanoscale circle and are connected by (generalized) stacking faults. Due to the complicated nonplanar structure of the split dislocation configuration and associated stacking faults, the split dislocation has a low mobility. Results of the model take into account experimental data on suppression of dislocation slip in Gum Metal reported in the literature.

DOI: [10.1103/PhysRevB.77.094115](https://doi.org/10.1103/PhysRevB.77.094115)

PACS number(s): 61.50.Lt, 62.20.D-, 71.20.Lp

I. INTRODUCTION

Partial and split dislocations are recognized as typical defects strongly influencing physical and mechanical properties of various solids such as nanocrystalline metals,¹⁻¹⁰ semiconductor quantum dots and wires,¹¹⁻¹⁶ semiconductor and metallic thin films,¹⁷⁻²⁰ and high-transition-temperature superconductors.²¹⁻²⁵ A conventional split dislocation represents a pair of partials that move in one crystallographic plane and are connected by a planar stacking fault. At the same time, there are examples of nonplanar splitting at which a preexistent perfect dislocation splits into three or more partials whose cores are not located on the same plane.²⁶ Also, perfect dislocations with cores of atomic-scale radius may spread into dislocations with large cores of nanoscale radius. For instance, dislocations with nanoscale disordered cores were experimentally observed in superconducting cuprates²⁷ and irradiated silicon.²⁸ Commonly, dislocation configurations with nonplanar split and spread cores are immobile.

Recently, a new group of alloys, called Gum Metal, with Ti-24 at. % (Ta+Nb+V)-(Zr-Hf)-O composition and remarkable properties has been developed.²⁹⁻³³ Gum Metal shows an unusual deformation behavior supposed to be crucially influenced by splitting of dislocations. In general, Gum Metal exhibits high strength, low Young's modulus, superelasticity (without martensitic transformations), excellent cold workability, and low resistance to shear in certain crystallographic planes.²⁹⁻³³ Plastic deformation starts in Gum Metal at applied stresses close to its ideal shear strength and occurs through the formation of large planar defects called giant faults. Each giant fault has thickness of around 1 nm and conducts very large local plastic strain of around thousands of percent or more. This special (dislocation-free) deformation through giant faults dominates in Gum Metal, while the conventional dislocation slip is suppressed. In particular, high resolution electron microscopy (HRTEM) characterization revealed paucity of conventional lattice dislocations with cores having atomic-scale diameters in deformed Gum Metal.²⁹⁻³³ A mechanism responsible for suppression of the conventional dislocation slip in Gum Metal is under discussion. Following Refs. 29 and 34, the solute hardening

effect of oxygen perhaps in the form of ZrO clusters can pin lattice dislocations. At the same time, if ZrO clusters are assumed to be impenetrable by lattice dislocations,³⁴ they should inhibit plastic shear carried by giant faults as well. However, following experimental data,²⁹⁻³³ Gum Metal is effectively deformed through giant faults. In this context, validity of the model^{29,34} is questionable, and there is motivation in searching for an alternative mechanism which can be responsible for the inhibition of dislocation mobility in Gum Metal. We think that nonplanar splitting of perfect lattice dislocations makes them immobile, in which case the conventional dislocation slip is suppressed in Gum Metal. The main aim of this paper is to theoretically describe the circular splitting transformation of lattice dislocations and discuss its effects on the dislocation mobility in Gum Metal.

II. GEOMETRY OF NONPLANAR SPLITTING OF SCREW DISLOCATIONS IN GUM METAL: MODEL ASSUMPTIONS

Let us consider the dislocation slip geometry in Gum Metal that commonly has a body centered cubic (bcc) crystal lattice structure. In general, the "pencil slip" is typical in bcc crystals²⁶ which occurs by screw dislocation movement in several slip systems, such as $\langle 111 \rangle \{110\}$, $\langle 111 \rangle \{112\}$, and $\langle 111 \rangle \{123\}$. The specific feature of bcc Gum Metal, differentiating it from conventional bcc crystals, is related to the fact that slip planes $\langle 111 \rangle \{110\}$, $\langle 111 \rangle \{112\}$, and $\langle 111 \rangle \{123\}$ are elastically softened in Gum Metal.²⁹⁻³³ More precisely, values of the shear modulus G in these slip planes are extremely low (G is around 9 GPa) compared to those in other planes.^{29-33,35} This specific feature is treated to be responsible for the existence of experimentally observed²⁹⁻³³ nanodisturbances—planar nanoscopic areas of local shear—in deformed Gum Metal. Following Ref. 31, nanodisturbances are effectively modeled as nanoscale dipoles of "noncrystallographic" partial dislocations with arbitrary, nonquantized Burgers vectors.

The existence of several elastically softened slip planes can also enhance the nonplanar splitting of perfect screw dislocations into conventional and noncrystallographic partials in Gum Metal. More precisely, a perfect lattice disloca-

tion in Gum Metal is expected to split into a dislocation configuration consisting of several partials that have different slip planes coinciding with elastically softened planes. In general, cores of the resultant partials are connected by a system of generalized stacking faults that hamper the movement of the partials. [A generalized stacking fault is a planar defect resulted from a cut of a perfect crystal across a single plane into two parts which are then subjected to a relative displacement through an arbitrary vector \mathbf{s} (lying in the cut plane) and rejoined.^{36–38} Its partial case is a conventional stacking fault corresponding to a displacement through a Burgers vector of a conventional partial dislocation.] Also, the splitting gives rise to the formation of a nanoscale region where the crystal lattice structure is highly violated at stacking faults and the chemical composition is different from that of the surrounding material. The latter is due to the effects of stress fields of the resultant partials on the chemical composition near their cores. According to the general theory of diffusion in strained alloys,³⁹ large (small) atoms of Gum Metal tend to move to the areas where tensile (compressive) stresses of the partials exist. In particular, oxygen-rich and -deficient areas are formed near preexistent lattice dislocations through diffusion of oxygen atoms. Elastic interaction of the partials with ensembles of inhomogeneously distributed oxygen atoms limits the mobility of the split dislocation. More than that, the discussed nanoscale region (containing both violations of the crystal lattice structure and the chemical composition inhomogeneities) can be treated as the large nanoscale core of the split dislocation in Gum Metal. This statement is indirectly supported by the HRTEM observation²⁹ of edge dislocations with nanoscale cores in Gum Metal [see central part of Fig. 2(c) presented in Ref. 29]. Mobility of dislocations with large cores is inhibited in Gum Metal due to the structural factor (but not only the above factor associated with chemical inhomogeneities at the dislocation cores). It is because the dislocation movement should be accompanied by transformations of the structure within the large dislocation core, while these transformations need to overcome energy barriers much larger than the conventional Peierls barrier for movement of perfect dislocations with atomic-scale cores.

Let us consider geometry of the dislocation splitting process in the exemplary case of a screw dislocation with Burgers vector $\mathbf{B}=(a/2)[111]$ (with a being the crystal lattice parameter) in Gum Metal. The direction $[111]$ along which both the Burgers vector and line of the considered screw dislocation are oriented plays the same role for screw dislocations having 12 easy slip systems (containing elastically softened direction $[111]$): $(1\bar{1}0)$, $(10\bar{1})$, $(01\bar{1})$, $(11\bar{2})$, $(1\bar{2}1)$, $(\bar{2}11)$, $(1\bar{2}\bar{3})$, $(21\bar{3})$, $(\bar{3}12)$, $(\bar{3}21)$, $(1\bar{3}2)$, $(2\bar{3}1)$. [For illustration, Figs. 1(a) and 1(b) show easy slip planes of the $\{110\}$ and $\{112\}$ types, respectively, containing elastically softened direction $[111]$.] Since a screw dislocation can move in any plane, it can split into partials moving in any slip system listed above. In conventional bcc metals, the dislocation splitting commonly occurs in planes of the type $\{112\}$ because the energy of stacking faults in these planes is lower compared to that in other planes. With this aspect taken into account, we will consider the nonplanar splitting of a screw

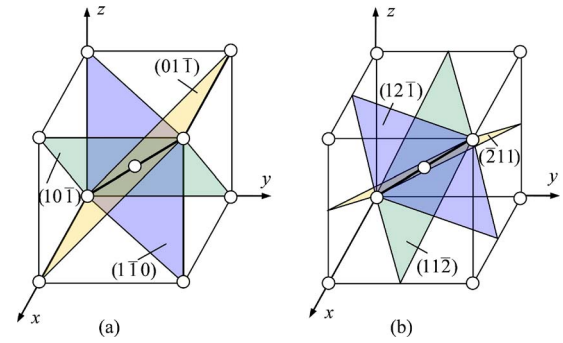


FIG. 1. (Color online) Crystallographic planes in bcc lattice contain elastically softened direction $[111]$ (bold line) and serve as planes where the splitting of a screw dislocation with the Burgers vector $\mathbf{B}=(a/2)[111]$ occurs. (a) Crystallographic planes of the $\{110\}$ type. (b) Crystallographic planes of the $\{112\}$ type.

dislocation into (i) 3 partials moving in planes $(11\bar{2})$, $(\bar{1}21)$, and $(\bar{2}11)$ [Fig. 2(a)], (ii) 6 partials consisting of three pairs moving along planes $(11\bar{2})$, $(1\bar{2}1)$, and $(\bar{2}11)$ with two partials moving in each plane [Fig. 2(b)], and (iii) 12 noncrystallographic partials moving in six planes—planes $(11\bar{2})$, $(1\bar{2}1)$, and $(\bar{2}11)$ of type $\{112\}$ as well as planes $(1\bar{1}0)$, $(10\bar{1})$, and $(01\bar{1})$ of type $\{110\}$ —with two partials moving in each plane [Fig. 2(c)]. Figure 2 presents the projection of the initial and split dislocation configurations on plane (111) , in which case the dislocation lines are perpendicular to this plane. Arrows show directions along which the partial dislocations move during the corresponding splitting transformations. The partial dislocations resultant from the splitting in planes of the $\{112\}$ and $\{110\}$ types move in directions $\langle 110 \rangle$ and $\langle 112 \rangle$, respectively.

Since studies of Gum Metal are in their infancy, there is deficit in experimentally verified information on its material and structural parameters. Many details of its structure and deformation behavior are still unknown. In these circum-

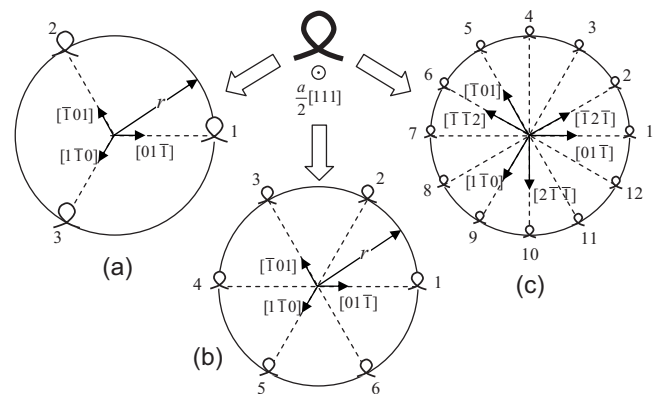


FIG. 2. Screw dislocation of $[111]$ type splits into (a) 3, (b) 6, and (c) 12 partials belonging to various slip planes. Generalized stacking faults (dashed segments) are formed which join the partials of the same slip system. Arrows show directions along which partial dislocations move during the corresponding splitting transformations.

stances, in order to theoretically describe the nonplanar splitting of screw dislocations and calculate (estimate) its critical parameters, we have to make several simplifying assumptions within our model. They are briefly as follows:

(i) Cores of partials resultant from the nonplanar splitting are located at a circle (Fig. 2). This assumption is rather natural because all the three split dislocation configurations shown in Fig. 2 are axially symmetric. More than that, the assumption is strictly correct, if values of the stacking fault energy in all the splitting planes of a split dislocation configuration are identical. The latter condition is valid, for the split dislocation configurations shown in Figs. 2(a) and 2(b). Each of these configurations is resulted from the splitting process occurring along the same set of crystallographic planes. At the same time, the condition is approximate for the dislocation configuration shown in Fig. 2(c) since it is resulted from the splitting process occurring along different crystallographic planes, namely, planes of the $\{112\}$ and $\{110\}$ types.

(ii) The resultant partials in all the situations (Fig. 2) are screw dislocations because this kind of splitting is more energetically favorable compared to other kinds.

(iii) In the calculation of energy characteristics of the nonplanar splitting (see Sec. III), we will use a first approximation representation³¹ of Gum Metal as an elastically isotropic solid characterized by the shear modulus G . In general, this assumption is rather natural because results of the isotropic elasticity calculations are correct enough in most problems of the theory of defects. In the partial case under consideration of this paper, we have shown that results of the isotropic elasticity calculations are weakly modified by accounting for anisotropy effects (see the Appendix).

(iv) As with Ref. 31, the value of the shear modulus G in isotropic elasticity calculations in Sec. III is taken as its minimum value $G=9$ GPa. In these circumstances, our theoretical examination operates with the minimum limit of the difference between the elastic energies (proportional to G) of the initial perfect and resultant partial dislocations. At the same time, the latter difference serves as the basic driving force for the nonplanar splitting (Fig. 2). As a corollary, our examination will give another strict criterion for the nonplanar splitting to occur.

(v) As with Ref. 31, the energy of generalized stacking fault is taken as a simple periodic function (sin) (for details, see Sec. III).

Assumptions (i)–(v) simplify a mathematical analysis of the problem under consideration but do not mask its key aspects.

Let us specify geometric parameters (Burgers vectors and spatial positions) of partials within our model of nonplanar splitting. Since the resultant partials are screw dislocations, all the splitting versions (Fig. 2) are described in terms of Burgers vectors as the following dislocation reaction: $(a/2) \times [111] = N(a/2N)[111]$, where N is the number of the resultant partials. In the case of splitting into three and six partials, their Burgers vectors are $(a/6)[111]$ [Fig. 2(a)] and $(a/12) \times [111]$ [Fig. 2(b)], respectively. Following Ref. 26, such partials are crystallographic ones. [Note that partials with Burgers vectors $(a/12)[111]$ [Fig. 2(b)] were observed in computer simulations (see Ref. 26 and references therein).

However, the authors are unaware about the experimental observation of such partials in real bcc metals.] The third version of the splitting of the perfect screw dislocations [Fig. 2(c)] results in the formation of 12 noncrystallographic partials with Burgers vectors of type $(a/24)[111]$, different from Burgers vectors of conventional partials. Since Burgers vectors $(a/6)[111]$ [Fig. 2(a)], $(a/12)[111]$ [Fig. 2(b)], and $(a/24)[111]$ [Fig. 2(c)] are not perfect lattice vectors, (generalized) stacking faults are formed between the partials composing pairs in each the splitting plane (see dashed segments in Fig. 2).

Following the model assumption (i), the partials are located at a circle with both radius r and center at the line of the initial screw dislocation (Fig. 2). Let us numerate the partials from 1 to N , starting from the partial at the direction $[01\bar{1}]$ and then moving counterclockwise, as shown in Fig. 2. For the dislocation reaction under consideration, the Burgers vector magnitudes of the partials (Fig. 2) are $s_i = a\sqrt{3}/2N$ ($i = 1, 2, \dots, N$). The position of each partial on the circle shown in Fig. 2 is specified by its vector radius \mathbf{r}_i . The vector \mathbf{r}_i connects the circle center and the i th partial dislocation core. In these circumstances, we have

$$\begin{aligned} \mathbf{r}_1 &= \frac{r}{\sqrt{2}}[01\bar{1}], & \mathbf{r}_2 &= \frac{r}{\sqrt{2}}[\bar{1}01], \\ \mathbf{r}_3 &= \frac{r}{\sqrt{2}}[1\bar{1}0] & \text{for } N=3 \text{ [Fig. 2(a)],} \end{aligned} \quad (1)$$

$$\begin{aligned} \mathbf{r}_1 &= -\mathbf{r}_4 = \frac{r}{\sqrt{2}}[01\bar{1}], & \mathbf{r}_2 &= -\mathbf{r}_5 = \frac{r}{\sqrt{2}}[\bar{1}01], \\ \mathbf{r}_3 &= -\mathbf{r}_6 = \frac{r}{\sqrt{2}}[1\bar{1}0] & \text{for } N=6 \text{ [Fig. 2(b)],} \end{aligned} \quad (2)$$

$$\begin{aligned} \mathbf{r}_1 &= -\mathbf{r}_7 = \frac{r}{\sqrt{2}}[01\bar{1}], & \mathbf{r}_2 &= -\mathbf{r}_8 = \frac{r}{\sqrt{6}}[\bar{1}2\bar{1}], \\ \mathbf{r}_3 &= -\mathbf{r}_9 = \frac{r}{\sqrt{2}}[\bar{1}10], \end{aligned}$$

$$\begin{aligned} \mathbf{r}_4 &= -\mathbf{r}_{10} = \frac{r}{\sqrt{6}}[\bar{2}11], & \mathbf{r}_5 &= -\mathbf{r}_{11} = \frac{r}{\sqrt{2}}[\bar{1}01], \\ \mathbf{r}_6 &= -\mathbf{r}_{12} = \frac{r}{\sqrt{6}}[\bar{1}\bar{1}2] & \text{for } N=12 \text{ [Fig. 2(c)].} \end{aligned} \quad (3)$$

Thus, we have all geometric parameters [in particular, Burgers vectors and spatial positions specified by formulas (1)–(3)] of partials to calculate energy characteristics of the nonplanar splitting of screw dislocations in Gum Metal. These characteristics will be examined in the next section.

III. ENERGY CHARACTERISTICS OF NONPLANAR SPLITTING OF SCREW DISLOCATIONS IN GUM METAL

The total energy change characterizing the circular splitting (Fig. 2) is given in its general form as follows:

$$\Delta W = W_1 - W_0, \quad (4)$$

where W_1 and W_0 are the energies of the final (split) and initial (nonsplit) dislocation configurations, respectively. The initial dislocation configuration represents a sole screw dislocation with Burgers vector $\mathbf{B}=(a/2)[111]$ (whose magnitude is equal to $B=a\sqrt{3}/2$). In the first approximation of Gum Metal as an elastically isotropic solid,³¹ the energy of the dislocation is given by the following well-known formula:²⁶

$$W_0 = \frac{GB^2}{4\pi} \left(\ln \frac{R}{B} + Z \right) = \frac{3Ga^2}{16\pi} \left(\ln \frac{2R}{a\sqrt{3}} + 1 \right), \quad (5)$$

where G denotes the shear modulus, R the screening length for the dislocation stress field, and Z the factor describing the energy of the dislocation core (hereinafter, we suppose $Z=1$).

The energy of the final (split) dislocation configuration is given as follows:

$$W_1 = \sum_{i=1}^N W_i^{el} + \frac{1}{2} \sum_{i=1}^N \sum_{\substack{j=1 \\ j \neq i}}^N W_{ij}^{int} + W_\gamma. \quad (6)$$

Here, W_i^{el} is the proper energy of the i th partial, W_{ij}^{int} is the energy that describes the interaction between the i th and j th partials, and W_γ denotes the sum energy of generalized stacking faults. For simplicity, as with Ref. 31, we represent the energy of a generalized stacking fault as the following periodic function of s (the magnitude of Burgers vector of a partial dislocation that bounds the generalized stacking fault) with period equal to $B=a\sqrt{3}/2$:

$$W_\gamma' = \gamma l \sin\left(\frac{\pi s}{B}\right). \quad (7)$$

Here, γ denotes the energy of conventional stacking fault and l the stacking fault length. In the cases under consideration (Fig. 2), there are N stacking faults of length $l=r$ and N partials whose Burgers vector magnitudes obey the following relationship: $s/B=1/N$. In this case, the sum energy W_γ of generalized stacking faults is given as

$$W_\gamma = N\gamma r \sin \frac{\pi}{N}. \quad (8)$$

Other terms on the right-hand side of formula (6) can be easily found using the standard theory of dislocations.²⁶ With these terms as well as formulas (1)–(8), after some algebra, we find the total energy change ΔW characterizing the circular splitting (Fig. 22) to be given as follows.

For $N=3$ [Fig. 2(a)],

$$\Delta W = -\frac{Ga^2}{16\pi} \left(\ln \frac{4r^2}{3a^2} + 2 \right) + \frac{3\sqrt{3}}{2} \gamma r. \quad (9)$$

For $N=6$ [Fig. 2(b)],

$$\Delta W = -\frac{5Ga^2}{32\pi} \left(\ln \frac{2r}{a\sqrt{3}} + 1 \right) + 3\gamma r. \quad (10)$$

For $N=12$ [Fig. 2(c)],

$$\Delta W = -\frac{11Ga^2}{128\pi} \left(\ln \frac{4r^2}{3a^2} + 2 \right) + 12\gamma r \sin \frac{\pi}{12}. \quad (11)$$

In accordance with formulas (9)–(11), the total energy change ΔW essentially depends on the stacking fault energy γ . As to our knowledge, there are no data on experimental measurements of γ in Gum Metal. In this case, we will estimate the energy γ of conventional nanoscale stacking faults, using characteristics of Gum Metal specimens deformed by macroscale giant faults. As shown in experiments,^{29–33} plastic deformation starts in Gum Metal through the formation of macroscale giant faults at applied stress $\sigma_f \approx 1$ GPa corresponding to the shear stress $\tau_f = \sigma_f/2 \approx 0.5$ GPa. Following a theoretical model,⁴⁰ macroscale giant faults are nucleated and developed from nanoscale generalized stacking faults bounded by noncrystallographic partials. That is, both structures and energies of conventional nanoscale stacking faults and macroscale giant faults are similar at least at the first stage of plastic flow in Gum Metal.⁴⁰ With these similarities taken into account, formation of a giant fault with plastic shear s under the shear stress τ is characterized by the energy change ΔW_{GF} (per unit area of the giant fault) approximately given as

$$\Delta W_{GF} \approx -\tau s + \gamma \sin(\pi s/B). \quad (12)$$

Here, the first term ($-\tau s$) specifies the shear stress work spent to plastic shear s and the second term [$\gamma \sin(\pi s/B)$] is the specific energy (per unit area) of the giant fault treated as a generalized stacking fault. Plastic flow is energetically favorable, if $d\Delta W_{GF}/ds < 0$ and unfavorable otherwise. In the case of a quasiequilibrium plastic deformation, we have $d\Delta W_{GF}/ds = 0$. With this equality and formula (12), we find the shear stress τ_f (measured in experiments^{29–33} as the shear stress causing plastic flow in Gum Metal) as the maximum value of τ . Since the generalized stacking fault structure periodically changes with period B , we have

$$\tau_f \approx \max \frac{d[\gamma \sin(\pi s/B)]}{ds} \quad \text{for } 0 \leq s \leq B. \quad (13)$$

Equation (13) yields $\gamma \approx \tau_f B / \pi$. As a corollary, we have the following estimate of the stacking fault energy in Gum Metal: $\gamma \approx 45$ mJ/m², for $\tau_f \approx 0.5$ GPa, and $B = a\sqrt{3}/2 \approx 0.29$ nm ($a = 0.33$ nm, see Ref. 34).

Also, note that, for the circular splitting (Fig. 2) in Gum Metal, the ideal crystal structure is violated within the circular region and its chemical composition can be different from that of the nondefect areas. Therefore, values of γ that characterize generalized stacking faults within the circular region can vary rather widely. In this context, in our further calculations, we will use various values of γ being in the wide range from 10 to 100 mJ/m².

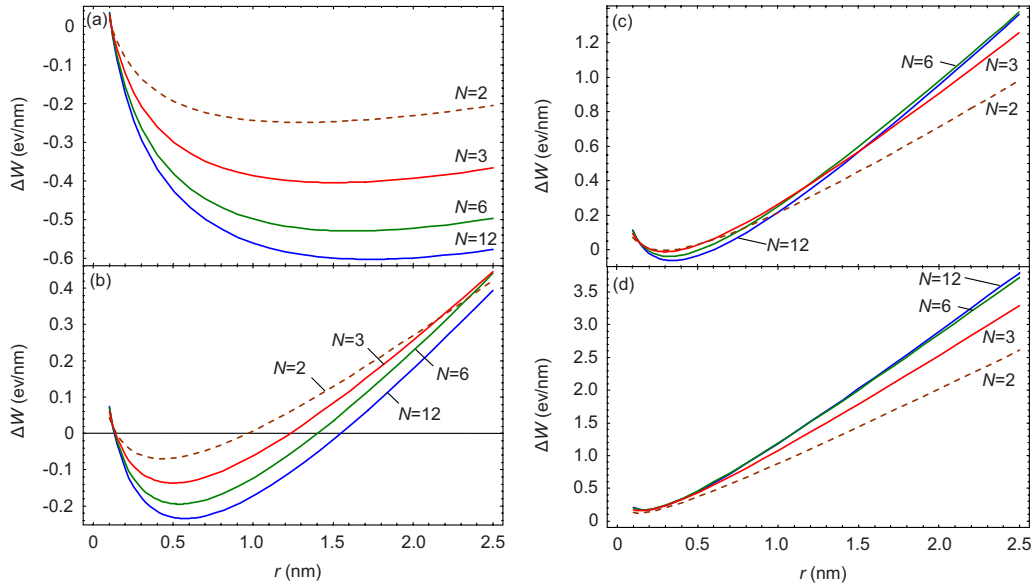


FIG. 3. (Color online) Dependences $\Delta W(r)$, for (a) $\gamma=10$ mJ/m², (b) $\gamma=30$ mJ/m², (c) $\gamma=50$ mJ/m², (d) $\gamma=100$ mJ/m², characterize the circular splitting of a screw dislocation of $[111]$ type into $N=3, 6$, and 12 partials and planar splitting into $N=2$ partials.

With formulas (9)–(11), we have calculated the dependences $\Delta W(r)$, for the three splitting versions shown in Fig. 3, various values of $\gamma=10, 30, 50$, and 100 mJ/m² [see curves in Figs. 3(a)–3(d), respectively], and the following typical values of other parameters of Gum Metal:^{32,34} $G=9$ GPa and $a=0.33$ nm. Figure 3 shows that the dependences $\Delta W(r)$ are negative (the circular splitting is energetically favorable) at $\gamma \leq 30$ mJ/m², for all the three splitting versions, and the splitting slightly enhances with increasing the number of resultant partials. Also, for comparison, Fig. 3 shows the dashed curve corresponding to the following planar splitting of a lattice screw dislocation into two screw partials:

$$\frac{a}{2}[111] = \frac{a}{3}[111] + \frac{a}{6}[111]. \quad (14)$$

This curve was calculated by formulas (4)–(8), with $N=2$, $s_1=a\sqrt{3}/3$, $s_2=a\sqrt{3}/6$, and $\mathbf{r}_1=-\mathbf{r}_2=(r/2)[01\bar{1}]$. [Planar splitting reactions for dislocations in bcc metals, discussed in Ref. 26, can be described in a first approximation by expression (14). Also, this reaction was mentioned in Ref. 41.] As it follows from Fig. 3, the planar splitting [Eq. (14)] is energetically unfavorable compared to nonplanar splitting versions shown in Fig. 2.

IV. CONCLUDING REMARKS

Thus, the nonplanar splitting of a perfect screw dislocation of the $\langle 111 \rangle$ type into three or more partials (Fig. 2) is energetically favorable in the reasonable range of parameters of Gum Metal. In doing so, each perfect dislocation splits into several partials having different slip planes (Fig. 2) coinciding with elastically softened planes. Cores of the resultant partials are connected by a system of (generalized) stacking faults that hamper the movement of the partials. In

general, the splitting results in the formation of a nanoscale circlelike region where the crystal lattice structure is highly violated at the stacking faults (Fig. 2) and the chemical composition is different from that of the surrounding material. The latter is due to the effects of stress fields of the resultant partials, producing compositional inhomogeneities near their cores. The elastic interaction of the partial dislocations with the compositional inhomogeneities in their vicinities limits the dislocation mobility. Also, the split dislocation movement is suppressed because it should be accompanied by high energy transformations of the structure within its large nanoscale core. Thus, split dislocation configurations become immobile and hardly contribute to plastic flow in Gum Metal. In this context, the nonplanar splitting of screw dislocations (Fig. 2) is capable of causing the experimentally observed^{29–33} inhibition of the conventional dislocation slip in Gum Metal. References 29 and 34 suggest an alternative explanation of low dislocation mobility through the solute hardening effect in Gum Metal. This effect is also capable of contributing to the experimentally observed^{29–33} inhibition of the conventional dislocation slip in Gum Metal. To identify the nature of the dislocation slip suppression and, in general, physical mechanisms responsible for the remarkable deformation behavior of Gum Metal, further experimental and theoretical studies in this area should be carried out.

ACKNOWLEDGMENT

The work was supported in part (for S.V.B and I.A.O) by a Research Agreement with Toyota Central R&D Laboratories.

APPENDIX

Let us estimate the anisotropy effect on results of our calculations of energies characterizing partial dislocations

(Fig. 2) in Gum Metal. In the context of this paper, we will focus our consideration on screw dislocations of $[111]$ type in bcc lattice. In the case of such dislocations, an analysis of the anisotropy effect is not complicated. Let us consider a screw dislocation of $[111]$ type in bcc lattice. The stress field of a screw dislocation of $[111]$ type in bcc lattice in the cylindrical coordinate system (r, θ, z) (associated with the straight dislocation line coinciding with axis z and oriented along $[111]$) is given as follows:²⁶

$$\sigma_{\theta z} = K_s \frac{b}{2\pi r}, \quad (\text{A1})$$

$$\sigma_{rz} = -\frac{K_s(M^2 - 1)}{\cot 3\theta + M^2 \tan 3\theta} \frac{b}{2\pi r}. \quad (\text{A2})$$

Here, b is the magnitude of the dislocation Burgers vector and K_s and M are the constant coefficients. These coefficients are in complicated relationships with elastic moduli C_{11} , C_{12} , and C_{44} (for details, see Ref. 26). The polar angle θ in formula (A2) has its zero at the $[\bar{1}\bar{2}\bar{1}]$ direction. Other components of the stress tensor are equal to zero.

A screw dislocation in an isotropic solid creates only the component $\sigma_{\theta z}$ of the stress tensor.²⁶ As a corollary, with the isotropic elasticity theory, the force of the interaction between two screw dislocations is strictly oriented along the line that connects the dislocation cores and is perpendicular to them. In accordance with formulas (A1) and (A2), in the cubic anisotropy approximation, an additional component σ_{rz} occurs which causes the force of the interaction between two screw dislocations to have a component perpendicular to the

line connecting the dislocation cores. In general, the energy of the elastic interaction between two screw dislocations changes, if the additional component σ_{rz} is taken into account. However, formula (A2) shows that $\sigma_{rz}=0$ at $\theta = m30^\circ$, where m is an integer. Actually, for the dislocation configurations presented in Figs. 2(a)–2(c), any pair of the screw dislocations is located in either the $\{110\}$ or $\{112\}$ plane. Each of the $\{110\}$ or $\{112\}$ planes makes angle $\theta = m30^\circ$ with the $[\bar{1}\bar{2}\bar{1}]$ direction.

Now, let us consider the proper elastic energy of dislocations. The proper energy depends on the only component $\sigma_{\theta z}$. From formula (A1), it follows that the component $\sigma_{\theta z}$ taking into account anisotropy is given by the expression²⁶ for $\sigma_{\theta z}$ in the isotropic situation, with the shear modulus G replaced by the coefficient K_s . That is, K_s serves as an effective shear modulus in the $[111]$ direction.

To summarize, all the expressions exploited in this paper in examination of the isotropic case are valid in the situation with a cubic anisotropy as well, if the shear modulus G is replaced by the coefficient K_s . The effect of the elastic softening is well pronounced in materials having an extremely low difference $C_{11}-C_{12}$.³⁵ Calculation of K_s , with data³⁵ of computer modeling of elastic moduli characterizing binary alloys taken into consideration, shows the value of K_s to be close to the value of $C_{11}-C_{12}$. In particular, for binary alloy $\text{Ti}_{0.75}\text{Ta}_{0.25}$, Ref. 35 has reported the following values of elastic constants (in units of GPa): $C_{11}=129.9$, $C_{12}=121.6$, $C_{44}=38.6$, and $C_{11}-C_{12}=8.2$. In doing so, one finds $K_s=9.1$ GPa. This value is very close to that (9 GPa) of the shear modulus G used in our calculations within the isotropic elasticity theory.

¹J. Schiøtz, T. Vegge, F. D. Di Tolla, and K. W. Jacobsen, Phys. Rev. B **60**, 11971 (1999).

²H. Van Swygenhoven, M. Spaczer, A. Caro, and D. Farkas, Phys. Rev. B **60**, 22 (1999).

³H. Van Swygenhoven and P. M. Derlet, Phys. Rev. B **64**, 224105 (2001).

⁴H. Van Swygenhoven, P. M. Derlet, and A. Hasnaoui, Phys. Rev. B **66**, 024101 (2002).

⁵M. Chen, E. Ma, K. J. Hemker, H. Sheng, Y. M. Wang, and X. Cheng, Science **300**, 1275 (2003).

⁶X. Z. Liao, F. Zhou, E. J. Lavernia, S. G. Srinivasan, M. I. Baskes, D. W. He, and Y. T. Zhu, Appl. Phys. Lett. **83**, 632 (2003).

⁷X. Z. Liao, F. Zhou, E. J. Lavernia, D. W. He, and Y. T. Zhu, Appl. Phys. Lett. **83**, 5062 (2003).

⁸T. Shimokawa, A. Nakatani, and H. Kitagawa, Phys. Rev. B **71**, 224110 (2005).

⁹S. V. Bobylev, M. Yu. Gutkin, and I. A. Ovid'ko, Phys. Rev. B **73**, 064102 (2006).

¹⁰M. Yu. Gutkin, I. A. Ovid'ko, and N. V. Skiba, Phys. Rev. B **74**, 172107 (2006).

¹¹H. Yamaguchi, J. G. Belk, X. M. Zhang, J. L. Sudijono, M. R. Fahy, T. S. Jones, D. W. Pashley, and B. A. Joyce, Phys. Rev. B **55**, 1337 (1997).

¹²K. Thillman and A. Forster, Thin Solid Films **368**, 93 (2000).

¹³J. Zou, X. Z. Liao, D. J. H. Cockayne, and Z. M. Jiang, Appl. Phys. Lett. **81**, 1996 (2002).

¹⁴I. A. Ovid'ko, Phys. Rev. Lett. **88**, 046103 (2002).

¹⁵I. A. Ovid'ko and A. G. Sheinerman, Phys. Rev. B **66**, 245309 (2002).

¹⁶I. A. Ovid'ko and A. G. Sheinerman, Adv. Phys. **55**, 627 (2006).

¹⁷D. Halley, Y. Samson, A. Marty, P. Bayle-Guillemaud, C. Beigné, B. Gilles, and J. E. Mazille, Phys. Rev. B **65**, 205408 (2002).

¹⁸V. Fournée, J. Ledieu, T. Cai, and P. A. Thiel, Phys. Rev. B **67**, 155401 (2003).

¹⁹J. Kioseoglou, G. P. Dimitrakopoulos, Ph. Komninou, H. M. Polatoglou, A. Serra, A. Béré, G. Nouet, and Th. Karakostas, Phys. Rev. B **70**, 115331 (2004).

²⁰D. N. Zakharov, Z. Liliental-Weber, B. Wagner, Z. J. Reitmeier, E. A. Preble, and R. F. Davis, Phys. Rev. B **71**, 235334 (2005).

²¹I.-F. Tsu, S. E. Babcock, and D. L. Kaiser, J. Mater. Res. **11**, 1383 (1996).

²²I.-F. Tsu, J.-L. Wang, D. L. Kaiser, and S. E. Babcock, Physica C **306**, 163 (1998).

²³H. Kung, J. P. Hirth, S. R. Foltyn, P. N. Arendt, Q. X. Jia, and M. P. Maley, Philos. Mag. Lett. **81**, 85 (2001).

²⁴M. Yu. Gutkin and I. A. Ovid'ko, Phys. Rev. B **63**, 064515 (2001).

- ²⁵S. V. Bobylev and I. A. Ovid'ko, Phys. Rev. B **67**, 132506 (2003).
- ²⁶J. P. Hirth and J. Lothe, *Theory of Dislocations* (Wiley, New York, 1982).
- ²⁷M. F. Chisholm and D. A. Smith, Philos. Mag. A **59**, 181 (1989).
- ²⁸D. Cherns, J. L. Hutchinson, M. L. Jenkins, P. B. Hirsch, and S. White, Nature (London) **287**, 314 (1980).
- ²⁹T. Saito, T. Furuta, J.-H. Hwang, S. Kuramoto, K. Nishino, N. Suzuki, R. Chen, A. Yamada, K. Ito, Y. Seno, T. Nonaka, H. Ikehata, N. Nagasako, C. Iwamoto, Y. Ikuhara, and T. Sakuma, Science **300**, 464 (2003).
- ³⁰T. Saito, T. Furuta, J.-H. Hwang, S. Kuramoto, K. Nishino, N. Suzuki, R. Chen, A. Yamada, K. Ito, Y. Seno, T. Nonaka, H. Ikehata, N. Nagasako, C. Iwamoto, Y. Ikuhara, and T. Sakuma, Mater. Sci. Forum **426**, 681 (2003).
- ³¹M. Yu. Gutkin, T. Ishizaki, S. Kuramoto, and I. A. Ovid'ko, Acta Mater. **54**, 2489 (2006).
- ³²T. Furuta, S. Kuramoto, J.-H. Hwang, K. Nishino, and T. Saito, Mater. Trans. **46**, 3001 (2005).
- ³³S. Kuramoto, T. Furuta, J.-H. Hwang, K. Nishino, and T. Saito, Metall. Mater. Trans. A **37**, 657 (2006).
- ³⁴T. Li, J. W. Morris, Jr., N. Nagasako, S. Kuramoto, and D. C. Chrzan, Phys. Rev. Lett. **98**, 105503 (2007).
- ³⁵H. Ikehata, N. Nagasako, T. Furuta, A. Fukumoto, K. Miwa, and T. Saito, Phys. Rev. B **70**, 174113 (2004).
- ³⁶V. Vitek, Philos. Mag. **18**, 773 (1968).
- ³⁷G. Lu, N. Kioussis, V. V. Bulatov, and E. Kaxiras, Phys. Rev. B **62**, 3099 (2000).
- ³⁸P. Lazar and R. Podloucky, Phys. Rev. B **75**, 024112 (2007).
- ³⁹L. A. Girifalco and D. O. Welch, *Point Defects and Diffusion in Strained Metals* (Gordon and Breach, New York, 1967).
- ⁴⁰M. Yu. Gutkin, T. Ishizaki, S. Kuramoto, I. A. Ovid'ko, and N. V. Skiba, Int. J. Plast. (to be published).
- ⁴¹R. W. K. Honeycomb, *The Plastic Deformation of Metals* (Edward Arnold, London, 1968).